8

# The effect of $H_2S$ on hydrogen and carbon black production from sour natural gas

[1]M. Javadi, [1]M. Moghiman and [2]Seyyed Iman Pishbin
[1]*Ferdowsi University of Mashhad,*
[2]*Khorasan Gas company*
*Iran*

## 1. Introduction

Hydrogen is well known as an ideal and clean source of energy which is believed to reduce the emission of carbon dioxide and therefore play a major role in decreasing the global warming problem [Ryu et al, 2007]. Eventual realization of a hydrogen economy requires cheap and readily available hydrogen sources and a technology to convert them into pure hydrogen in an efficient and sustainable manner [Abdel et al, 1998]. In addition to water that is an ideal hydrogen source, $CH_4$ and $H_2S$ are considered as alternative sources of hydrogen [Jang et al, 2007; T-Raissi, 2003]. On the other hand, there is ample scope for $CH_4$ and $H_2S$ as the raw source of $H_2$, because the energy required for $CH_4$ and $H_2S$ splitting ($\Delta H_{CH4}$=74.9 kJ/mol and $\Delta H_{H2S}$=79.9 kJ/mol) is much less than water splitting ($\Delta H_{water}$= 284.7 kJ/mol) [Jang et al, 2007]. There are several convenient technologies for production of $H_2$ from $CH_4$, including steam methane reforming (SMR), partial oxidation, pyrolysis, autothermal pyrolysis, and autothermal SMR [Huang & T-Raissi, 2007a]. Methane decomposition is a moderately endothermic reaction. It requires much less thermal energy (only 37.8 kJ per mol of hydrogen produced) than SMR (69 kJ/mol $H_2$). Besides, the decrease in the required energy, the $CO_2$ emission is also decreased in this method. Methane which is the main component of the high quality natural gas can be decomposed to hydrogen and carbon black in pyrolysis reactors [Abanades & Flamant , 2007; Moghima & Bashirnezhad, 2007]. Carbon black is an industrial form of soot produced by subjecting hydrocarbon feedstock to extremely high temperatures in a carefully controlled combustion process. Carbon black is widely used as filler in elastomers, tires, plastics and paints to modify the mechanical, electrical and optical properties of materials in which it is used [Ghosh, 2007; Petrasch et al, 2007].

As the prices of fossil fuel increase, abundant sour natural gas, so called sub-quality natural gas resources become important alternatives to replace increasingly exhausted reserves of high quality natural gases for the production of hydrogen and carbon black [Huang & T-Raissi, 2007b; Abdel et al, 1998]. At oil flow stations it is common practice to flare or vent SQNG, which is produced along with crude oil. This accounts for more than 100 million cubic meters ($m^3$) world-wide per day, and approximately equals to France's annual gas consumption [Gruenberger et al, 2002]. Clearly this is of considerable concern in terms of

global resource utilization and climate change implications. Gas flaring has also been blamed for environmental and human health problems such as acid rain, asthma, skin and breathing diseases [Lambert et al, 2006]. The removal of $H_2S$ from sub-quality natural gas is expensive and not commercially viable for large-scale plants. When $H_2S$ concentration in natural gas is higher than about 1.0%, the high separation cost makes the sour natural gas uneconomical to use [Huang & T-Raissi, 2007b]. As mentioned above, production of hydrogen and carbon black from sour natural gas is one viable option utilizing this untapped energy resource while at the same time reducing carbon oxides and hydrogen sulfide emissions.

There is a massive back ground literature on thermal decomposition of high quality natural gas using different types of reactors. Petrasch & Steinfeld (2007) have studied hydrogen production process using solar reactors with SMR method. Abanades & Flamant (2007) also have investigated the effect of different parameters and system geometry on methane conversion and hydrogen yield using thermal decomposition method in solar reactors. Their results show that the solar reactor producing pure $H_2$ has high efficiency in $CH_4$ conversion. Cho et al (2009) have studied on the development of a microwave plasma-catalytic reaction process to produce hydrogen and carbon black from pure natural gas. The direct conversion of methane, using various plasma technologies has widely been studied in order to obtain more valuable chemical products. Gruenberger et al (2002) and Moghiman & Bashirnezhad (2007) have investigated the effect of feedstock parameters on methane decomposition in carbon black furnace.

Although many studies have been carried out on high quality natural gas pyroysis, sour natural gas pyrolysis have received much less attention. Towler & Lynn (1996) introduced thermal decomposition of hydrogen sulfide at high temperature as an alternative of Clause process. The main advantage of the thermal decomposition is reduction of produced tail gas rather than Clauses process. They have investigated the effect of $CO_2$ presence in feed gas and temperature on decomposition and sulfur compounds production. Also, Huang and T-Raissi et al (2007b, 2007c and 2008) have performed the thermodynamic analyses of hydrogen production from sub-quality natural gas using a Gibbs reactor operation in the AspenPlusTM chemical process simulator. Javadi and Moghiman (2010) have investigated carbon disulfide, hydrogen and solid carbon production from sub-quality natural gas. Their results show that the maximum yield of C(s) is in 1000 °K and then decreases due to increasing of CS2 production.

Based on the importance of sub-quality natural gas pyrolysis, the effects of feedstock parameters, reactor temperature and $H_2S/CH_4$ molar ratio of feedstock on decomposition process have been studied using the proposed carbon black furnace by Gruenberger et al (2002).

## 2. Gas furnace carbon black

Hydrogen and carbon black production via thermal decomposition of natural gas have been achieved using a carbon black furnace [Gruenberger et al, 2000 & 2002], plasma [Gaudernack & Lynum 1998], solar radiation [Abanades et al, 2007 & 2008], a molten metal bath and thermal reactors with and without catalyst [Steinberg, 1998; Ishihara et al, 2002; Muradov et al, 1998 & Kim et al, 2004].

Depending on the way that heat is supplied to sour natural gas, carbon black furnaces can be classified as follows:

Type 1: Part of the natural gas or any other fuel burns inside the reactor to provide heat needed to decompose the sour natural gas.

Type 2: Direct heat transfer from inert hot gases introduced into the reactor. This method is known as "Hydrogen Sulfide- Methane Reformation".

The carbon black furnace used in this investigation is a small-scale axial flow reactor identical to that reported previously by Gruenberger et al (2002). The furnace has been designed on the basis of using gaseous fuels as feedstock hydrocarbon, with a maximum output of 10 kg carbon black per hour. The basic geometry of the carbon black furnace is shown in Fig. 1, consisting of a pre-combustor, a mixing zone and a reactor. In the pre-combustor, the axially injected natural gas burns with inlet air introduced through two tangential inlets. Then, the highly swirling hot combustion gases mix with the sub-quality natural gas injected radially into the pre-combustor in the proximity of the mixing zone. A sudden increase in the tube diameter at the exit of the choke promotes vigorous mixing of the SQNG fuel with the hot gases leading to thermal decomposition of $CH_4$+$H_2S$ and formation of hydrogen, carbon black, sulfur compounds and other precursor species for the formation of carbon black [Lockwood et al, 1995].

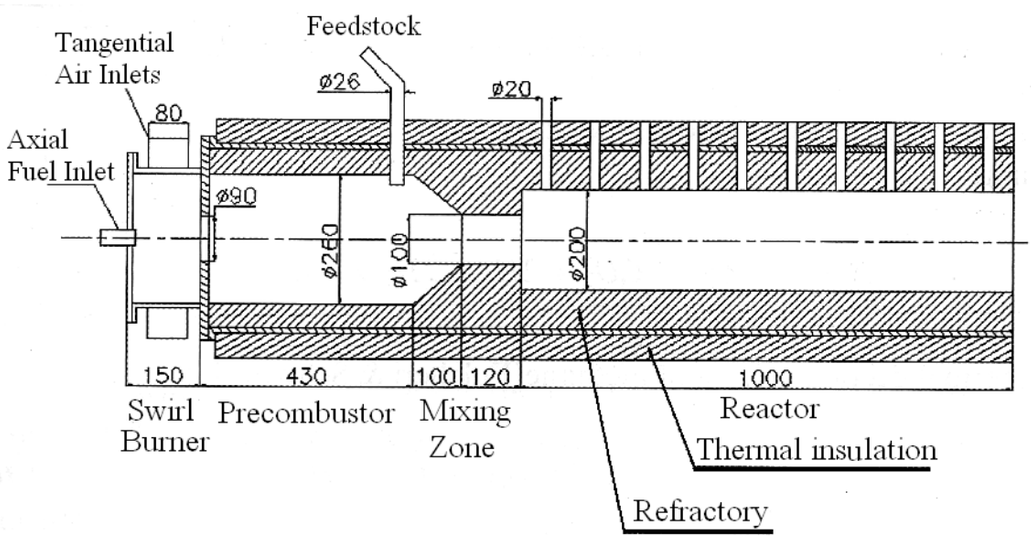


Fig. 1. Carbon black gas furnace[Gruenberger et al, 2002]

## 3. Chemical reaction modelling

Production of carbon black through thermolysis of SQNG involves a complex series of chemical reactions which control conversion of both $CH_4$ and $H_2S$ as follows [Huange & T-Raissi, 2007b; Towler & Lynn, 1996]:

$$CH_4 \rightarrow C(S) + 2H_2 \qquad \Delta H^{\circ}_{298} = -74.9\,kJ/mol \qquad \text{Reaction (1)}$$

$$H_2S \rightarrow \frac{1}{2}S_2 + H_2 \qquad \Delta H^{\circ}_{298} = -79.9\,kJ/mol \qquad \text{Reaction (2)}$$

Since reaction 1 is mildly endothermic, it requires temperatures higher than $850^{\circ}K$ to proceed at reasonable rates [Dunker et al, 2006], and, as reaction 2 is highly endothermic, temperatures in excess of $1500^{\circ}K$ is required for achieving reasonable rates [Huang & T-Raissi, 2008].
Under special circumstances including using catalyst $H_2S$ can react with methane producing carbon disulfide ($CS_2$) and $H_2$ [Huange & T-Raissi, 2008].

$$2H_2S + CH_4 \Leftrightarrow CS_2 + 4H_2 \qquad \Delta H^{\circ}_{298K} = 232\,kJ/mol \qquad \text{Reaction (3)}$$

A portion of $CH_4$ and $H_2S$ can oxidize to produce $CO$, $CO_2$ and $SO_2$ [ Abdel et al, 1998]:

$$CH_4 + \frac{1}{2}O_2 \rightarrow CO + H_2 + H_2O \quad \text{and} \quad CO + \frac{1}{2}O_2 \rightarrow CO_2 \qquad \text{Reaction (4)}$$

$$H_2S + \frac{3}{2}O_2 \rightarrow SO_2 + H_2O \qquad \text{Reaction (5)}$$

$H_2S$ can also react with $CO_2$ producing $COS$ [Sakanishi et al, 2005]:

$$H_2S + CO_2 \Leftrightarrow COS + H_2O \qquad \text{Reaction (6)}$$

## 4. Turbulence–chemistry interaction

The mixture fraction/PDF method is used to model the turbulent chemical reactions occurring in the diffusion, combustion and thermal decomposition of natural gas in the carbon black furnace. This method, which assumes the chemistry is fast enough for a chemical equilibrium to always exist at molecular level, enables handling of large numbers of reacting species, including intermediate species. Transport equations are solved for the mean mixture fraction $\bar{f}$, its variance $\overline{f'^2}$ and for enthalpy $\bar{h}$. Calculations and PDF integrations are performed using a preprocessing code, assuming chemical equilibrium between 30 different species. The results of the chemical equilibrium calculations are stored in look-up tables which relate the mean thermochemical variables (species mass fractions, temperature and density) to the values of $\bar{f}$, $\overline{f'^2}$ and $\bar{h}$ [Saario & Rebola, 2005].
In non-adiabatic systems, where change in enthalpy, due to heat transfer, affects the mixture state, the instantaneous thermo chemical state of the mixture, resulting from the chemical equilibrium model, is related to a strictly conserved scalar quantity known as the mixture fraction, f, and the instantaneous enthalpy, $H^*, \phi_i = \phi_i(f, H^*)$. The effects of turbulence on the thermo chemical state are accounted for with the help of a probability density function (PDF):

$$\bar{\phi}_i = \int_0^1 \phi_i(f, \overline{H}^*) p(f) df. \tag{1}$$

In this work, the $\beta$-probability density function is used to relate the time-averaged values of individual species mass fraction, temperature and fluid density of the mixture to instantaneous mixture fraction fluctuations. The $\beta$-PDF in terms of the mean mixture fraction $\bar{f}$ and its variance $\overline{f'^2}$, can be written as:

$$P(f) = \frac{f^{\alpha-1}(1-f)^{\beta-1}}{\int_0^1 f^{\alpha-1}(1-f)^{\beta-1} df}, \quad 0 < f < 1 \tag{2}$$

where:

$$\alpha = \bar{f}\left[\frac{\bar{f}(1-\bar{f})}{\overline{f'^2}} - 1\right], \; \beta = (1-\bar{f})\left[\frac{\bar{f}(1-\bar{f})}{\overline{f'^2}} - 1\right]. \tag{3}$$

Using the unweighted averaging [Jones & Whitelaw, 1982], the values of the two parameters $\bar{f}$ and $\overline{f'^2}$ at each point in the flow domain are computed through the solution of the following conservation equations [Warnatz, 2006]:

$$\frac{\partial}{\partial x}(\rho u_i \bar{f}) = \frac{\partial}{\partial x_i}\left(\frac{\mu_t}{\sigma_t}\frac{\partial \bar{f}}{\partial x_i}\right), \tag{4}$$

$$\frac{\partial}{\partial x}(\rho u_i \overline{f'^2}) = \frac{\partial}{\partial x_i}\left(\frac{\mu_t}{\sigma_t}\frac{\partial \overline{f'^2}}{\partial x_i}\right) + C_g \mu_t \left(\frac{\partial \bar{f}}{\partial x_i}\right)^2 - C_d \rho \frac{\varepsilon}{k}\overline{f'^2}, \tag{5}$$

where the constants $\sigma_t$, $C_g (= 2/\sigma_t)$ and $C_d$ take the values 0.7, 2.86 and 2.0, respectively. The distribution of the instantaneous enthalpy is calculated from a transport equation as follows:

$$\frac{\partial}{\partial x}(\rho u_i \overline{H^*}) = \frac{\partial}{\partial x_i}\left(\frac{k_t}{c_p}\frac{\partial \overline{H^*}}{\partial x_i}\right) + \tau_{ik}\frac{\partial u_i}{\partial x_k} + S_h \tag{6}$$

where $k_t$ is turbulent thermal conductivity and $S_h$ includes the heat generated by the chemical reaction and radiation. The instantaneous enthalpy is defined as:

$$H^* = \sum_j m_j H_j = \sum_j m_j \left[\int_{T_{ref,j}}^{T} c_{p,j} dT + h_j^\circ(T_{ref,j})\right] \tag{7}$$

where $m_j$ is the mass fraction of species j and $h_j^\circ(T_{ref,j})$ is the formation enthalpy of species j at the reference temperature $T_{ref,j}$.

## 5. Numerical solution procedure

Fluent CFD software has been used to model the furnace employing solution-adaptive grid refinement technique to solve the 3D problem. Gambit preprocessor is used for the fully three dimensional geometry creations and unstructured grid generation. The 3D volume grid is represented in Fig 2. The domain is discretized into a grid of 20493 nodes and 82745 tetrahedral cells.

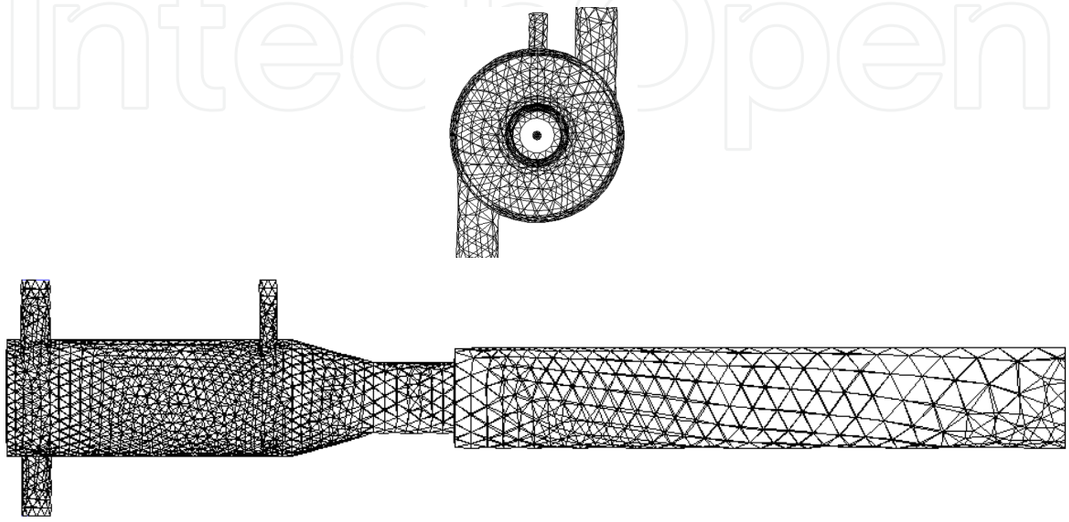

Fig. 2. Three-dimensional tetrahedral grid

The conservation equations for mass, momentum, energy, Reynold's stresses, dissipation rate, mixture fraction and its variance, and concentration of soot are solved by finite-volume analysis, using a second-order upwind scheme for discretisation of the convective terms in the transport equations.

The radiative heat transfer in the absorbing, emitting and scattering medium is calculated by the Discrete Ordinates (DO) radiation model [Murthy & Mathur, 1998]. The RSM (Reynolds stress model) is used for prediction of anisotropic, highly swirling and recirculating flow inside the combustor. Abandoning the isotropic eddy-viscosity hypothesis, the RSM closes the Reynolds-averaged Navier-Stokes equations by solving six differential transport equations for Reynolds stresses, together with an equation for the dissipation rate of turbulence kinetic energy. The conventional wall-function approach is used in the near-wall region. At the inlet boundary, conditions are specified once and did not need updating during the course of the solution procedure. At the outlet boundary, zero gradient conditions are applied. We assumed an isothermal boundary condition at the wall of the furnace.

A grid dependence study was conducted to arrive at the appropriate size of the grid for optimal accuracy and efficiency. The number of grid points was varied from 17231 to 36387 for typical set operating conditions. We observed that the field quantities varied less than 1% after the number of grid points increased beyond 20493. For the radiation model, emissivity coefficient at the flow inlets and outlets were taken to be 1.0 (black body absorption). Wall emissivity was set at 0.6, a typical value for combustion gases.

## 6. Results and discussion

As mentioned above, the processes of methane pyrolysis differ mainly by the way heat is supplied to the furnace. In this study, sour natural gas decomposition in a carbon black furnace has been investigated for two types of supplying heat. In the first type, the natural gas burns inside the pre-combustor (Fig.1) to provide required heat for decomposing feed sour gas. In this case, the problem is the effect of combustion product (process gases) and excess air which extremely affect on sour natural gas decomposition and furnace product. In the second type the heat transfers from inert hot gases to feed sour gas. In this case only reactions 1 to 3 are involved and there is not the problem of excess air and combustion products. In this study the sour natural gas thermal decomposition inside the axial flow gas furnace designed by Gruenberger et al (2002) has investigated. The results of two types of supplying heat for pyrolysis are as follows:

### 6.1 Type 1: Pyrolysis by hot combustion gases

The total pre-combustor inlet airflow rate is $19\times10^{-3}\,m^3/s$, at the temperature of 690° K and pressure of 1 bar. The equivalence ratio used for the pre-combustor is 0.92. The accuracy of the quantitative or even the qualitative trends for the combustion and decomposition parameters depend on the accuracy with which the temperature and species concentration fields are determined from the numerical calculation of the present model. To establish the accuracy of our model, we have been calculated and compared the model predictions to the experimental measurements of Gruenberger [Gruenberger et al, 2002] with no $H_2S$. For comparison purposes, we first conducted computations without $H_2S$ in feed gas.

A comparison of reactor outlet average temperature and carbon black yield (kg carbon black/kg feedstock) predicted by this model and by experimental results is given in Figs. 3 and 4. Results of Fig. 3 depict that the model predicts lower temperatures than the experimental data, especially at high feed flow rates. The discrepancy between the two results might be due to the fundamental assumption made in the combustion model (PDF fast chemistry combustion model), which assumes that chemistry is fast enough for a chemical equilibrium. Results of Fig. 4 show that the predicted and measured carbon black yields are in very good agreement and maximum carbon black yield is reached at the equivalence ratio of 3. The discrepancy between the two results can be attributed to the temperature levels obtained by the two methods (see Fig. 3). The lower temperature levels computed by the model might be due to higher decomposition of $CH_4$. Fig. 5 presents the calculated distributions for $CH_4$, $H_2S$, temperature and mass fraction of soot, carbon black, COS and gaseous sulfur predicted by the model at feed rate of $3\times10^{-3}\,kg/s$. $H_2S$ mass fraction in natural gas is assumed to be 10%. Of particular interest are Figs. 5d-f that show soot formation due to incomplete combustion of inlet methane and production of solid carbon and gaseous sulfur by pyrolysis of methane- hydrogen sulfide jet interaction with hot surroundings. Results from the model calculations seem to indicate that the use of more inlet injection ports for SQNG feed would increase the yield of carbon black and sulfur compounds.

Fig. 6 shows the reactor outlet temperature as a function of inlet mass flow rate for two cases a) with $H_2S$, b) without $H_2S$. It can be seen that the results obtained for these two cases are similar. The small discrepancy between the results may be due to $CH_4$ decomposition

reaction that begins at lower temperatures than that of $H_2S$. Also, Fig. 6 depicts that temperature drops precipitously with increasing flow rate of feed gas due to the endothermic nature of both $CH_4$ and $H_2S$ decompositions.

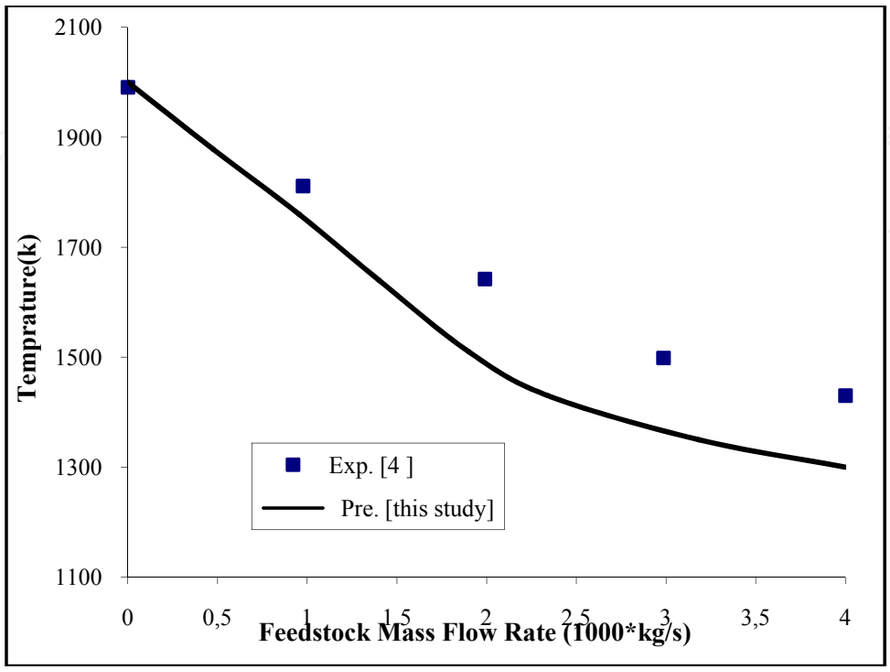


Fig. 3. Comparison of the predicted reactor outlet temperature with the experimental data

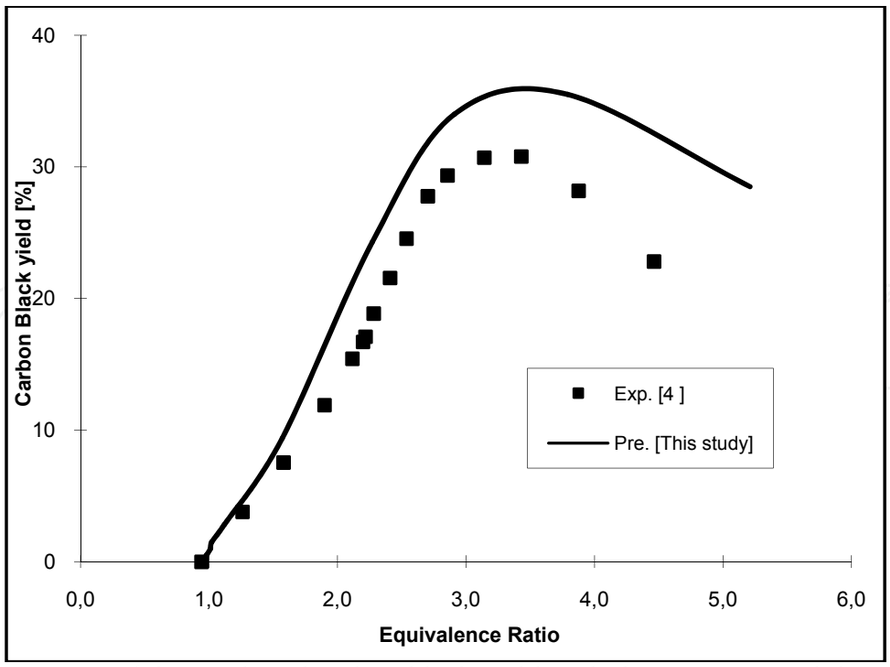


Fig. 4. Comparison of the predicted carbon black yield with the experimental data

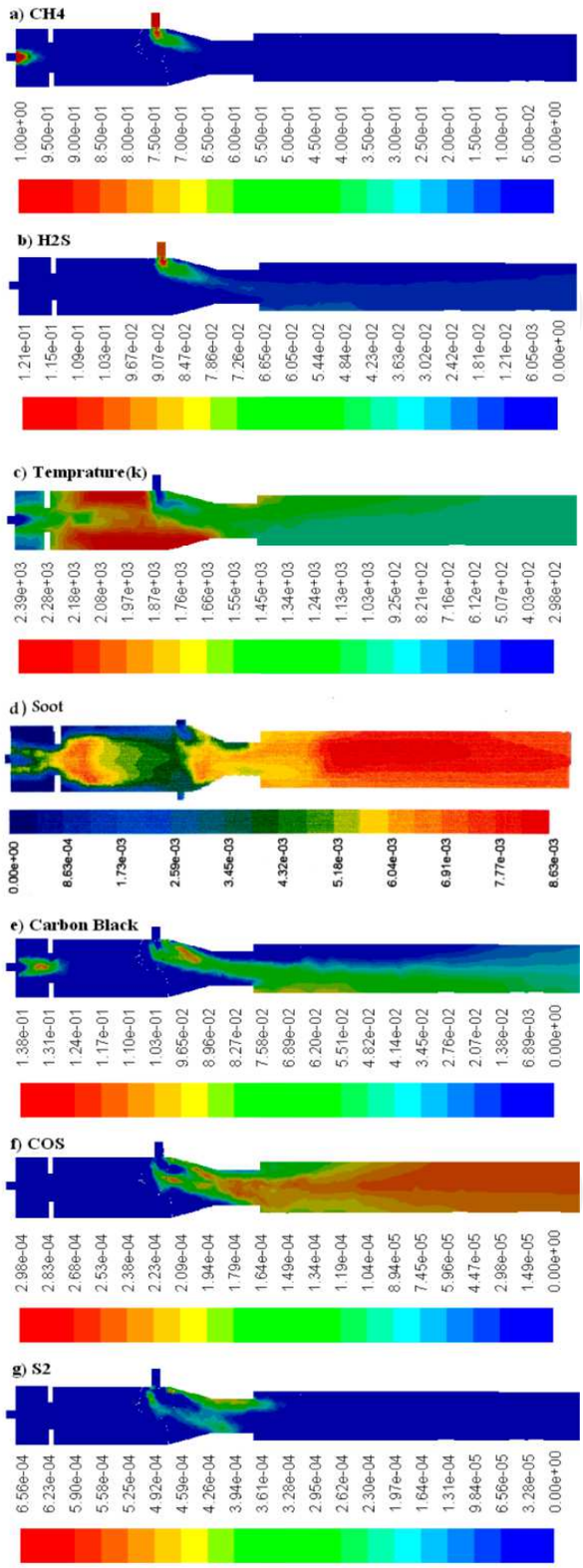


Fig. 5. Contour of species mass fractions and temperature (K)

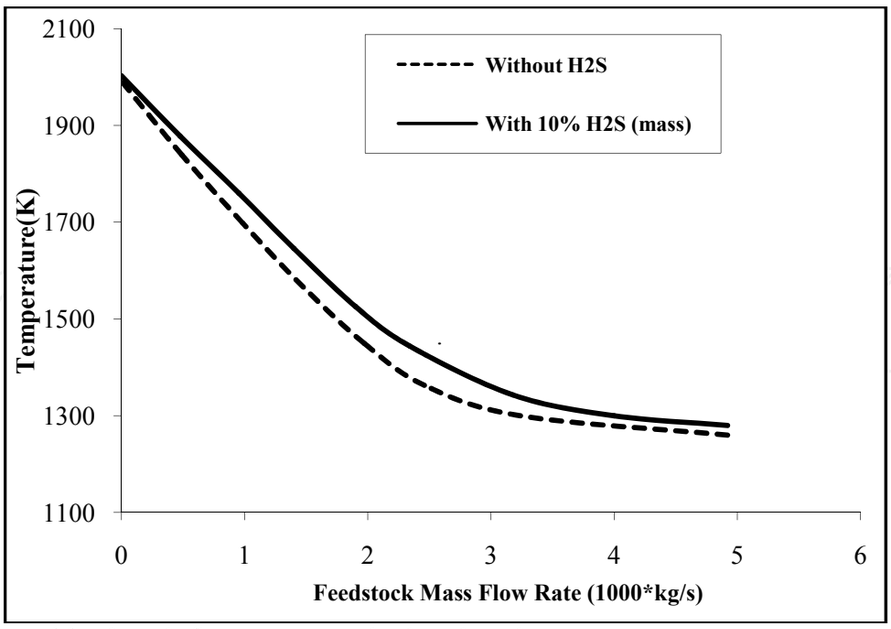


Fig. 6. Effect of feedstock flow rate on calculated outlet temperature

Figs. 7 and 8 show the effect of feed gas flow rate and reactor outlet temperature on $CH_4$ and $H_2S$ conversions given by [Huang & T-Raissi, 2008]:

$$CH_4 \text{ conversion} = \frac{[CH_4]_0 - [CH_4]}{[CH_4]_0} \times 100 \text{ , } H_2S \text{ conversion} = \frac{[H_2S]_0 - [H_2S]}{[H_2S]_0} \times 100$$

where $[CH_4]_0$ and $[H_2S]_0$ denote the initial (input) concentration of $CH_4$ and $H_2S$, respectively. $[CH_4]$ and $[H_2S]$ are equilibrium concentration of $CH_4$ and $H_2S$ at reactor outlet, respectively. Fig. 7 depicts that the $H_2S$ conversion drops sharply with increased feed gas flow rate, which can be attributed to the endothermic nature of $H_2S$ and $CH_4$ decomposition reactions. For higher values of feed gas flow rate $(\geq 0.002 kg/s)$ $CH_4$ conversion decreases with increased feed gas flow rate due to the endothermicity of $CH_4$ thermolysis. The major factor influencing $CH_4$ and $H_2S$ conversions appears to be temperature. Fig. 8 shows that $CH_4$ conversion reaches 100% at temperatures above $1100^\circ K$. Because $CH_4$ decomposition reaction is mildly endothermic, the temperature must be above $850^\circ K$ for the reaction to proceed at a reasonable rate. This is in accordance with the results of Huang and T-Raissi (2008). At any temperature, $H_2S$ conversion is less than that of $CH_4$, especially at those below $1300^\circ K$ wherein $H_2S$ conversion is less than 5%. For higher values of reactor temperature $(\geq 1300^\circ K)$, $H_2S$ conversion increases sharply with reaction temperature. As the reaction of $H_2S$ decomposition is endothermic, the temperature must be above $1500^\circ K$ for the reaction to proceed at rapid rates.

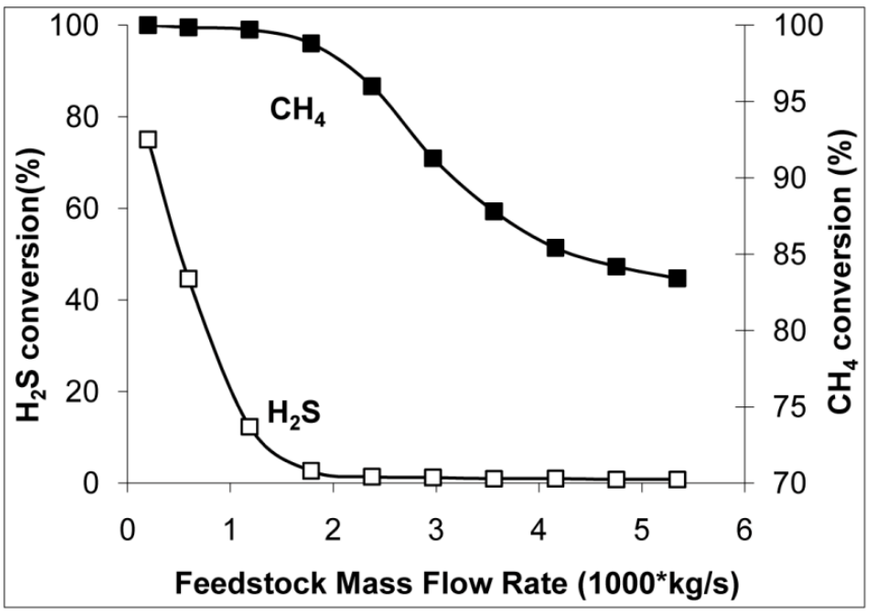


Fig. 7. Effect of feedstock mass flow rate on $H_2S$ and $CH_4$ conversions

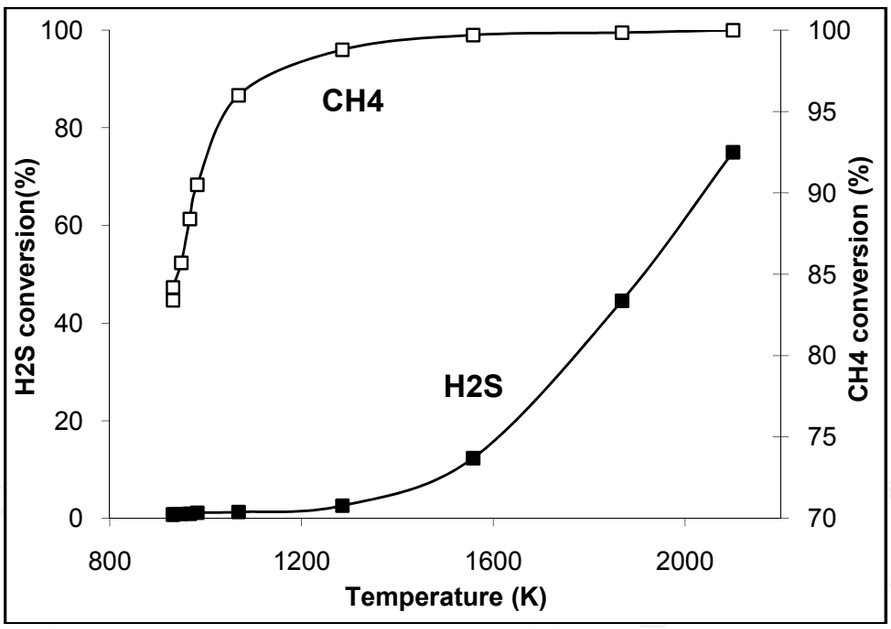


Fig. 8. Effect of reactor outlet temperature on $H_2S$ and $CH_4$ conversions

Figs. 9 shows the effect of feedstock flow rate on $CH_4$, carbon black, soot and CO mass fractions at the furnace outlet. It can be seen that for lower values of feed gas flow rates, the very high temperature pre-combustor effluent (see Fig. 6) causes the feedstock methane to convert to CO rather than carbon. For higher values of feedstock flow rate, the formation of carbon black increases, and due to the resulting lower temperatures, the mass fraction of CO and soot decreases. This is so because the soot model strongly depends on the reaction temperature. Fig. 10 shows the effect of feedstock flow rate on $H_2$ and carbon black yields at

the furnace outlet. It can be seen that the yield of $H_2$ increases with increased feed gas flow rate until it reaches a maximum value, and then drops with further increase in the flow rate. For higher values of feedstock flow rate, the yield of carbon black increases and due to reduction in CH4 conversion (see Fig. 7) the yield of hydrogen decreases.

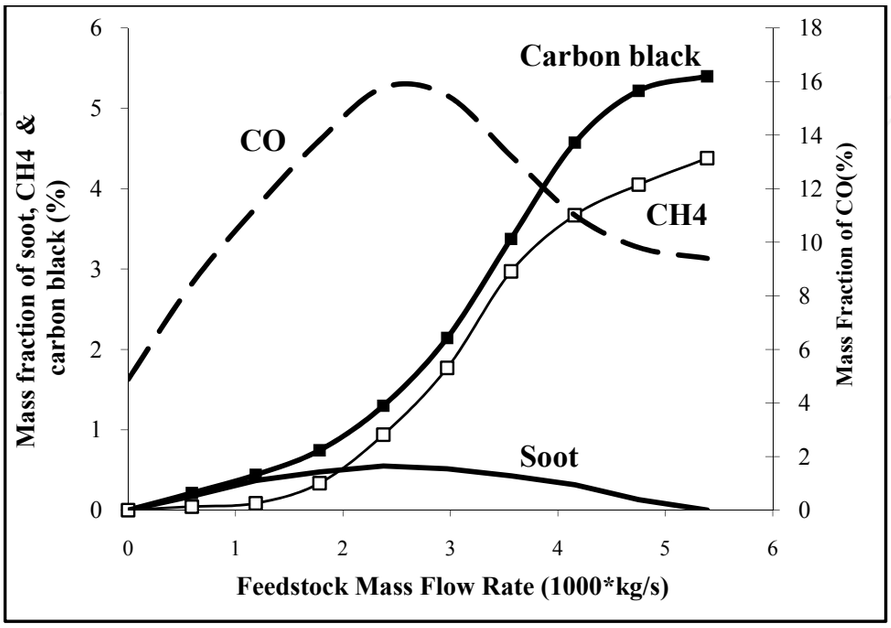


Fig. 9. Effect of feedstock flow rate on $CH_4$, CO, carbon black, and soot mass fractions

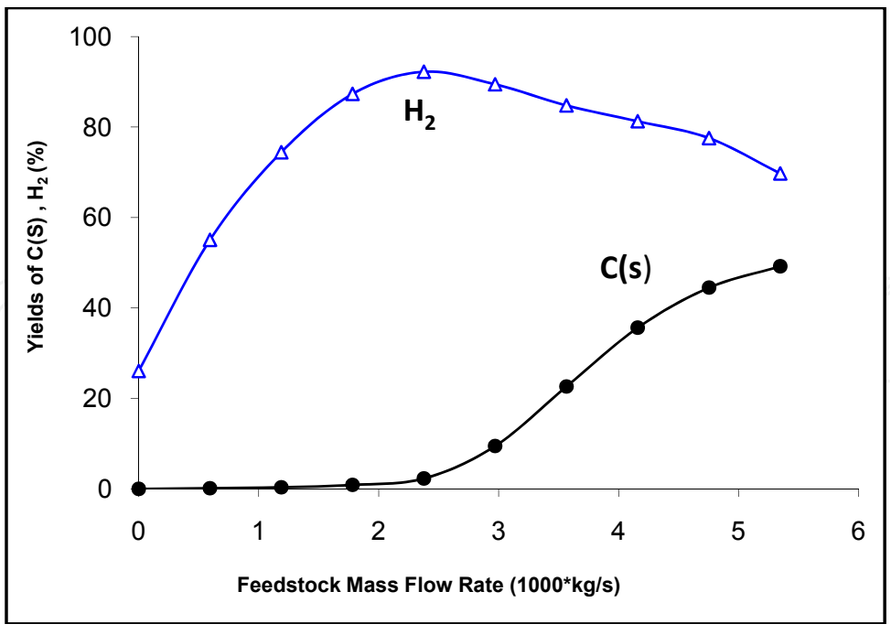


Fig. 10. Effect of feedstock mass flow rate on $H_2$ and C(S) productions

Fig. 11 depicts the yield of sulfur (due to $H_2S$ decomposition) and $SO_2$ (due to $H_2S$ combustion) as a function of feedstock flow rate at the outlet of the furnace. $S_2$ and $SO_2$ yields are defined as [Huang & T-Raissi, 2008]:

$$S_2(\%) = \frac{2[S_2]}{[H_2S]_0} * 100 \ , \ SO_2(\%) = \frac{[SO_2]}{[H_2S]_0} * 100 \, .$$

where $[S_2]$ and $[SO_2]$ denote the equilibrium molar concentrations of $S_2$ and $SO_2$, respectively. The figure reveals that for low values of feedstock flow rate $(\leq 0.002 kg/s)$ that result in high reaction temperatures (see Fig. 3) $H_2S$ converts mostly to $S_2$ and $SO_2$. It can be seen that for higher values of feedstock flow rate, yield of $S_2$ and $SO_2$ are quite low. This is due to reduced of $H_2S$ conversion (see Fig. 7). Figs. 12 and 13 depict the effects of feedstock mass flow rate and temperature on the yield of $COS$ and $CS_2$, respectively, as defined by:

$$COS(\%) = \frac{[COS]}{[H_2S]_0} * 100 \ , \ CS_2(\%) = \frac{[CS_2]}{[CH_4]_0} * 100$$

where $[COS]$ and $[CS_2]$ denote the equilibrium molar concentration of COS and $CS_2$, respectively [Huang & T-Raissi, 2008]. Fig. 12 shows that $COS$ and $CS_2$ yields increase with increased feedstock flow rate until they reach a peak, and then drop with further increase in feed gas flow rate. Figs. 12 reveals that yield of $CS_2$ is always low $(\leq 0.0007\%)$. This is in accord with results of Huang &T-Raissi (2008) and Towler & Lynn (1996).

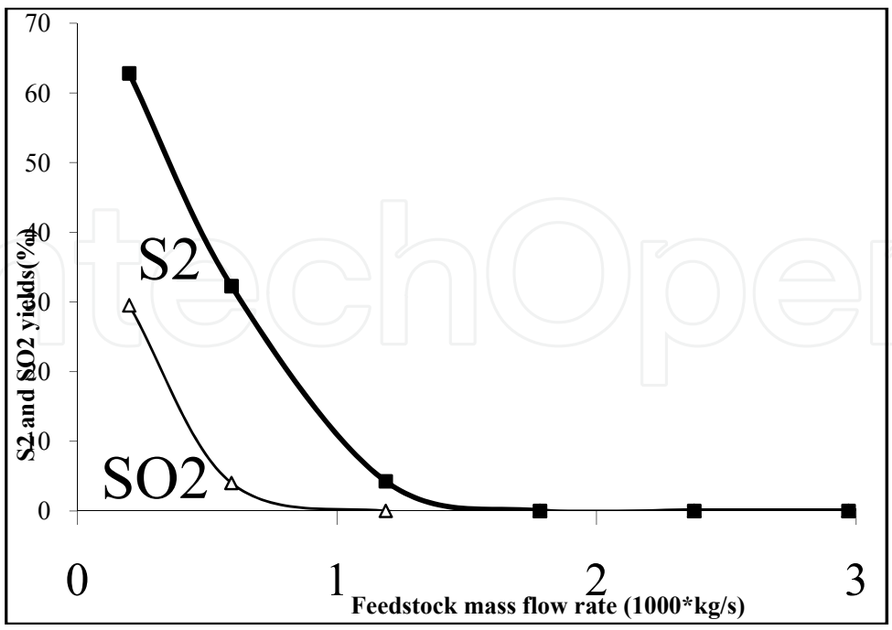


Fig. 11. Effect of feedstock mass flow rate on $S_2$ and $SO_2$

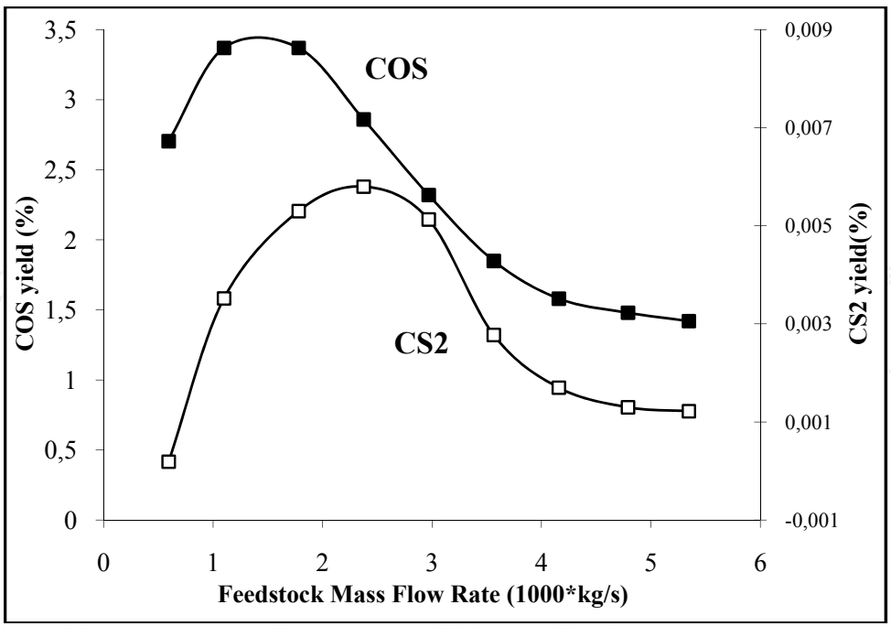


Fig. 12. Effect of feedstock mass flow rate on COS and $CS_2$ yields

### 6.2 Type 2: pyrolysis by inert hot gases

In the case of Type 2, the inert hot gas (argon) flow rate introduced into the pre-combustor is $3\times10^{-3}\,kg/s$ with pressure of 1 bar and the temperature varying from 600° K to 1800° K. The feedstock sour natural gas feed rate is $19\times10^{-3}\,m^3/s$ with $H_2S/CH_4$ molar ratio varying from 0 to 4 and the temperature of 300° K. As the reactions of $CH_4$ and $H_2S$ decomposition are endothermic, in order to avoid the reduction of inert gas temperature some thermal elements have been utilized.

Figs. 13 and 14 illustrate the effects of feedstock $H_2S/CH_4$ ratio and reaction temperature on $CH_4$ and $H_2S$ conversions. Results show that the major factor influencing $CH_4$ and $H_2S$ conversions is temperature. As the temperature increases, $CH_4$ conversion also increases to reach 100% at temperatures above 1100° K for $H_2S/CH_4$ feed ratio ranging from 0 to 4. Since the endothermic reaction of $CH_4$ conversion occurs at lower temperatures compared with $H_2S$ conversion, the reactor temperature is significantly affected by $CH_4$ molar ratio in feedstock. Based on these results it can be concluded that as the reaction temperature increases up to about 1100° K, methane pyrolysis is the dominant reaction that controls reactor temperature. $H_2S$ decomposition is the limiting step in the $H_2S$-methane reformation process (Reaction 3) as it proceeds by the sequential reaction involving $H_2S$ pyrolysis to form sulfur diatomic gas ($S_2$) (Reaction 2), followed by $S_2$ reaction with $CH_4$ to produce carbon disulfide ($CS_2$) and $H_2$. Fig. 15 depicts that $H_2$ production increases by increasing molar ratio of $CH_4$ (decreasing $H_2S/CH_4$ ratio) in feedstock and temperature. The rate of hydrogen production from pyrolysis of methane is much more than that of hydrogen sulfide. Therefore, any reduction in $H_2S/CH_4$ feed ratio, for constant feedstock mass flow rate, leads to significant increase in hydrogen production rate.

Figs. 16 and 17 depict the yields of carbon and sulfur as a function of $H_2S$ /$CH_4$ feed ratio and reaction temperature. Fig. 16 shows that carbon yield increases with increasing

temperature until the yield reaches a maximum value (at about 1000°K), and then drops with further increase in the temperature for $H_2S/CH_4$ ratios more than zero.

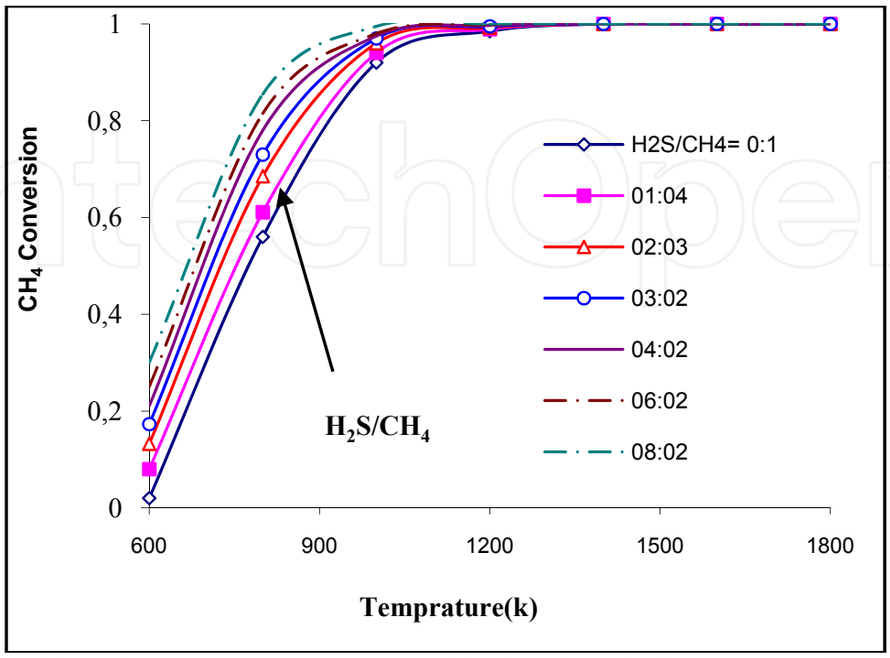


Fig. 13. The effect of reaction temperature and feedstock $H_2S/CH_4$ ratio on $CH_4$ conversion for constant feedstock mass flow rate in the case of Type 2

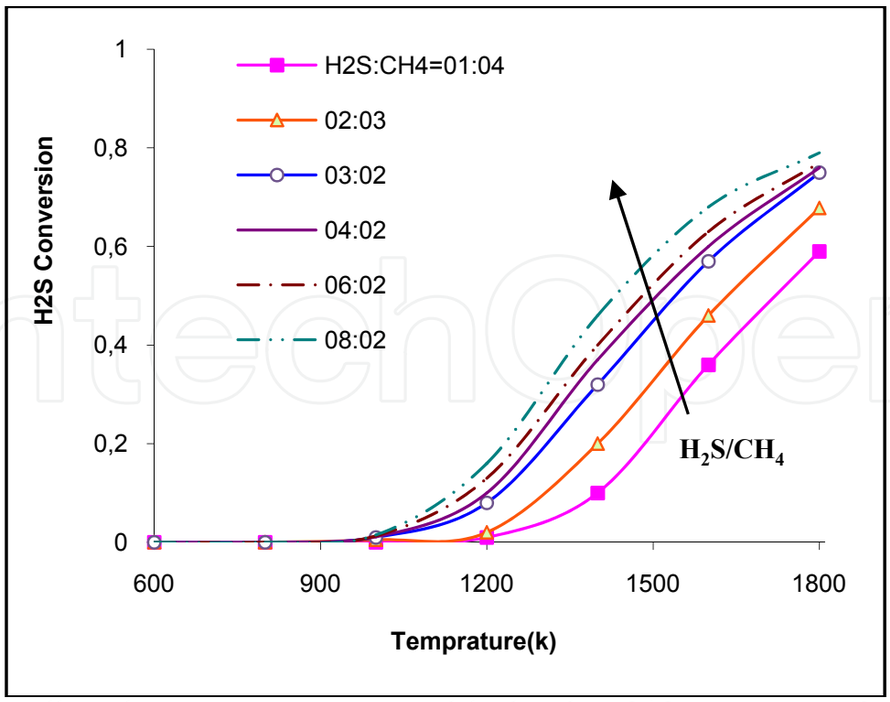


Fig. 14. The effect of reaction temperature and feedstock $H_2S/CH_4$ ratio on $H_2S$ conversion for constant feedstock mass flow rate in the case of Type 2

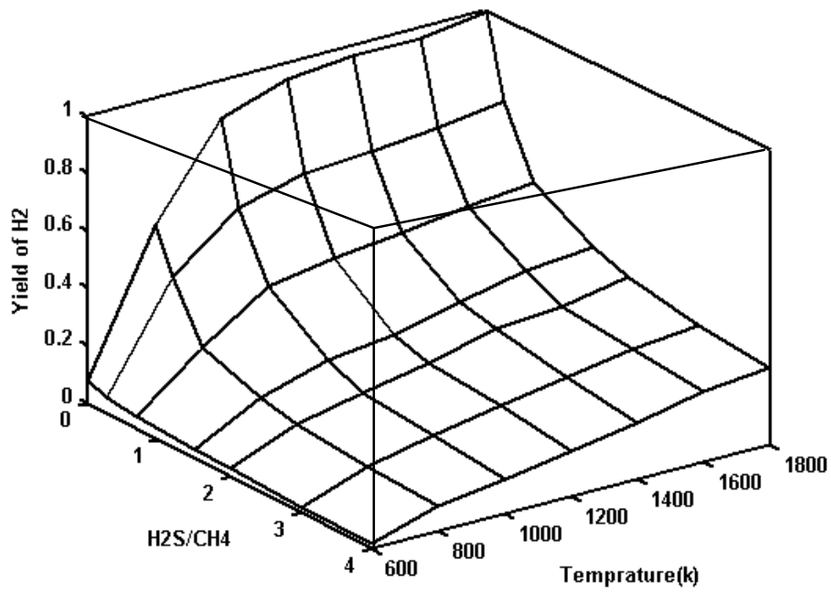


Fig. 15. Yield of $H_2$ as a function of reaction temperature and $H_2S/CH_4$ ratio for constant feedstock mass flow rate

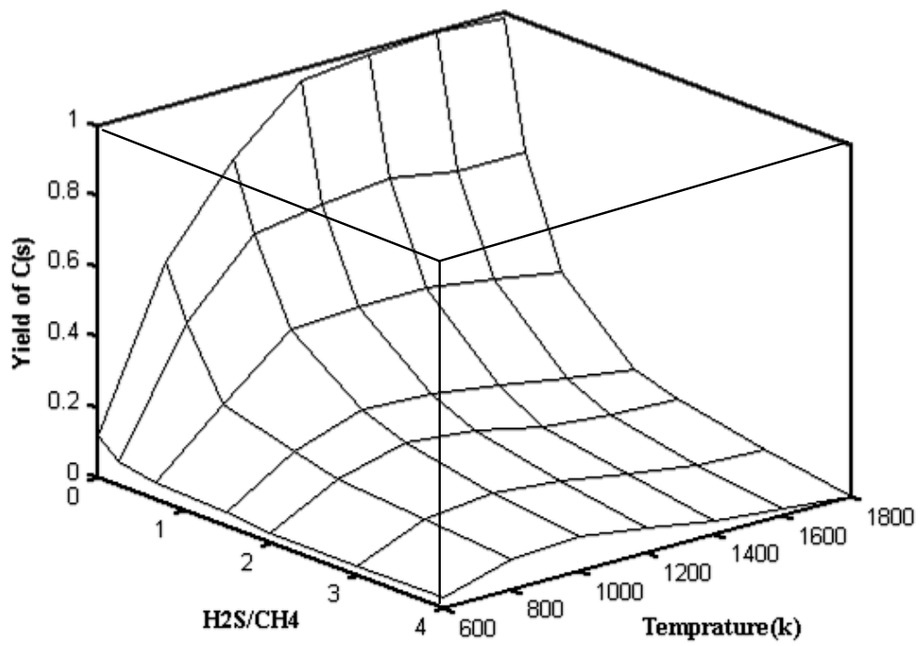


Fig. 16. The effects of temperature and $H_2S/CH_4$ ratio on C(s) yield for constant feedstock mass flow rate

In temperatures lower than 1000°K, hydrogen and carbon are produced by $CH_4$ decomposition. But in temperatures more than 1000°K hydrogen is produced from both of methane and hydrogen sulfide, and formed solid carbon from $CH_4$ decomposition is consumed by $CS_2$ production (Fig. 18). Fig. 17 depicts that by either increasing $H_2S/CH_4$ ratio or the reaction temperature, $S_2$ yield increases. As explained in chemical reactions section, hydrogen sulfide requires high temperatures to be decomposed. Consequently, $S_2$ yield for temperatures lower than 1000°K is negligible. As shown in Fig .18 , $CS_2$ yield depend not only on the temperature, but also on the $H_2S/CH_4$ feed ratio. In temperatures lower than 1000°K, the yield of carbon disulfide ($CS_2$) approaches zero (Fig. 7). These results are in accordance with results of Huang and T-Raissi (2008).

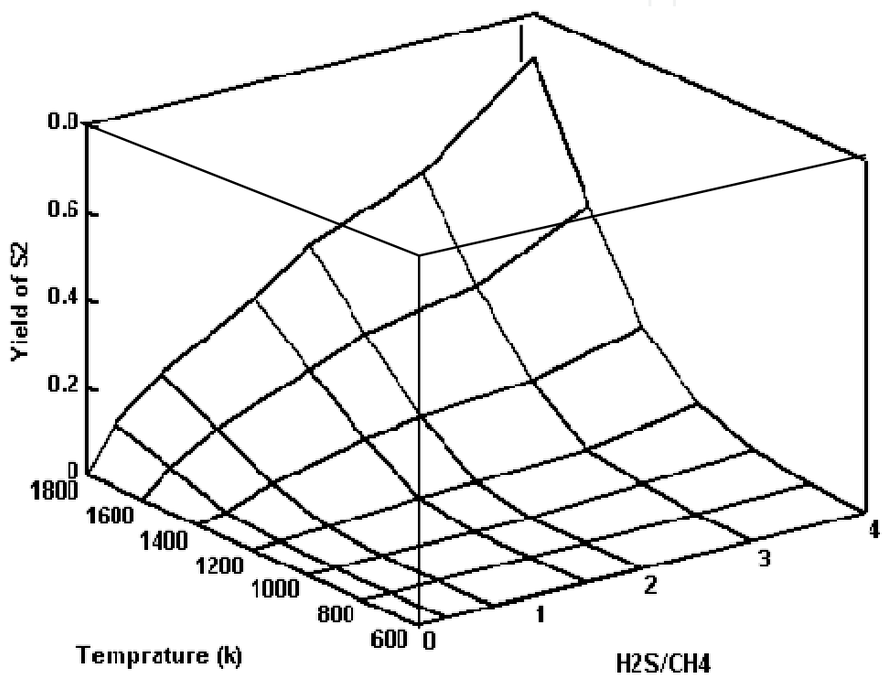


Fig. 17. The effects of reaction temperature and $H_2S/CH_4$ ratio on $S_2$ yield for constant feedstock mass flow rate

## 7. Conclusions

The production of hydrogen and carbon black from sub-quality natural gas containing methane ($CH_4$) and hydrogen sulfide ($H_2S$) has been analyzed for two types of supplying heat. Based on the presented results, the following conclusions may be drawn:

- The major factor influencing $CH_4$ and $H_2S$ conversions is reactor temperature.
- At temperatures above 1100°K, $CH_4$ conversion is complete.
- At any temperature, $H_2S$ conversion is less than that of $CH_4$, especially at temperature below 1300°K for which $H_2S$ conversion is less than 5%.
- For lower values of feedstock flow rate, $CH_4$ is converted to mostly CO and consequently, the yield of carbon black is low. For higher values of feed gas mass flow rates yield of carbon black increases to a maximum value before dropping at much higher feed gas flow rates.

- The yield of hydrogen (in combustion case) increases with increasing feed gas mass flow rate until it peaks and then drops with further increase in the flow rate.
- For temperatures higher than 1200°K, $H_2S$ conversion increases sharply with temperature.
- Since $CH_4$ conversion occurs at lower temperatures compared with $H_2S$ conversion, the reactor temperature is significantly affected by the amount of $CH_4$.
- The carbon yield reaches a maximum value about 1000°K and the then drops with further increase in the temperature for sour natural gas ($H_2S/CH_4$ ratio>0).
- CS2 and COS are minor products in combustion case and can be neglected, while CS2 yield in inert gas case reaches up to 80% as a major product.

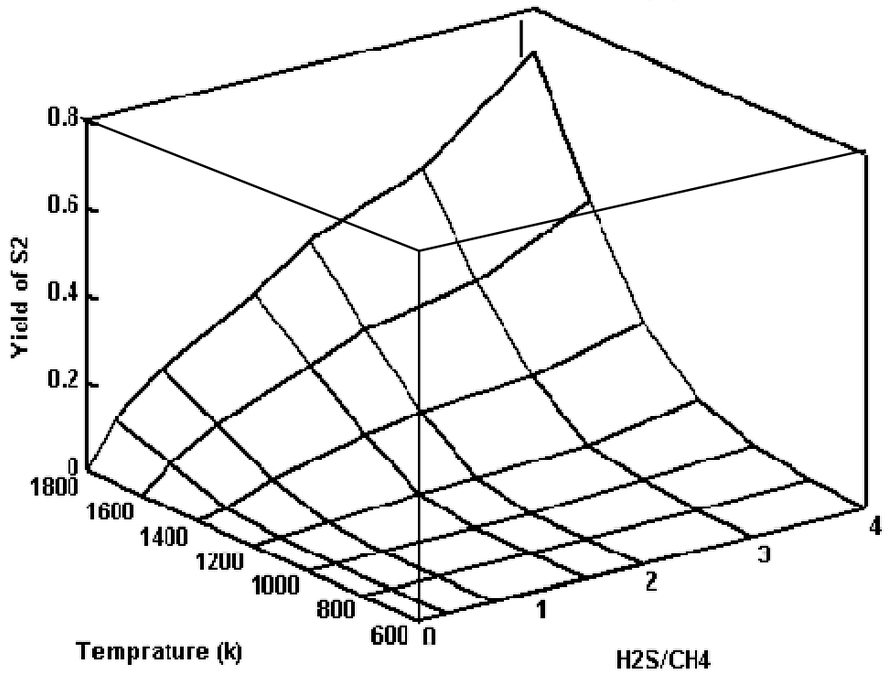


Fig. 18. The effects of reaction temperature and $H_2S/CH_4$ ratio on $CS_2$ yield for constant feedstock mass flow rate

## 8. References

Abanades, S. ; Flamant, G. (2007). Experimental study and modeling of a high-temperature solar chemical reactor for hydrogen production from methane cracking, *International journal of hydrogen energy*, Vol.32, 2007, pp. 1508-1515, ISSN:0360-3199

Abanades, S. & Flamant, G. (2008). Hydrogen production from solar thermal dissociation of methane in a high temperature fluid-wall chemical reactor, *Journal of Chemical engineering and processing* 47, 490–498, ISSN : 0255-2701

Abdel, H. K. ; Shalabi, M. A. ; AL-Harbi D. K. & Hakeem, T. (1998). Non catalytic partial oxidation of sour natural gas , *International journal. of hydrogen energy,* Vol. 23, pp. 457-462, ISSN:0360-3199

Brookes, S. J. and Moss, J. B. (1998). Predictions of soot and thermal radiation properties in confined turbulent jet diffusion flames. Journal of Combustion and Flame, Vol. 116, 1998, pp. 486-503,

Cho, W. ; Lee, S. H. ; Ju, W. S. & Baek, Y. (2004). J. K. Lee, Conversion of natural gas to hydrogen and carbon black by plasma and application of plasma carbon black, *Journal of catalysis today*, Vol. 98, pp. 633–638, ISSN: 0920-5861

Dunker, A. M. ; Kumar, S. & Mulawa, P. A. (2006). Production of hydrogen by thermal decomposition of methane in a fluidized-bed reactor—Effects of catalyst, temperature, and residence time, *International journal of hydrogen energy*, Vol.31, pp. 473-484, ISSN:0360-3199

Gaudernack, B. & Lynum, S. (1998). Hydrogen from natural gas without release of $CO_2$ to the atmosphere. *International journal of hydrogen energy*, Vol. 23, No. 12, pp. 1087-1093, ISSN:0360-3199

Ghosh, U. (2007). The Role of Black Carbon in Influencing Availability of PAHs in Sediments, *Journal of human and ecological risk assessment*, Vol. 13, pp. 276-285, ISSN: 1080-7039

Gruenberger, T. M.; Moghiman, M.; Bowen, P. J. & Syred, N. (2000). Improving mixing behaviour in new design of carbon black furnace using 3D CFD modeling, *5th European conference on industrial furnaces and boilers*, 972-8034-04-0, Porto, Portugal, April 2000.

Gruenberger, T. M.; Moghiman, M.; Bowen, P. J. & Syred, N. (2002). Dynamic of soot formation by turbulent combustion and thermal decomposition of natural gas, *Journal of Combustion science and technology,* Vol.174, pp.67-86, ISSN:0010-2202

Huang, C. & T-Raissi, A. (2007a). Analyses of one-step liquid hydrogen production from methane and landfill gas, *Journal of power sources,* Vol.173, pp. 950–958, ISSN: 0378-7753

Huang, C. & T-Raissi, A. (2007b). Thermodynamic analyses of hydrogen production from sub-quality natural gas, Part I: Pyrolysis and autothermal pyrolysis, *Journal of power sources*, Vol.163, pp. 645–652, ISSN:0378-7753

Huang, C. & T-Raissi, A. (2007c). Thermodynamic analyses of hydrogen production from sub-quality natural gas, Part II: Steam reforming and autothermal steam reforming, *Journal of power sources,* Vol. 163, pp.637–644, ISSN:0378-7753

Huang, C. & T-Raissi, A. (2008). Liquid hydrogen production via hydrogen sulfide methane reformation, *Journal of power sources,* Vol.175, pp. 464-472, ISSN:0378-7753

Ishihara, T.; Kawahara, A.; Fukunaga, A.; Nishiguchi, H.; Shinkai, H.; Miyaki, M. & Takita, Y. (2002). $CH_4$ decomposition with a Pd-Ag hydrogen-permeating membrane reactor for hydrogen production at decreased temperature, *Industrial & Engineering Chemistry Research,* Vol. 41, No.14, pp. 3365–3369, ISSN: 0888-5885

Jang, J.S.; Kim, H.G.; Borse, P. H. & Lee, J. S. (2007). Simultaneous hydrogen production and decomposition of $H_2S$ dissolved in alkalinewater over $CdS.TiO_2$ composite photocatalysts under visible light irradiation, *International journal of hydrogen energy*, Vol.32, pp. 4786-4791, ISSN:0360-3199

Javadi, M. Moghiman, M. (2010). Hydrogen and carbon black production from thermal decomposition sour natural gas, *international journal of spray and combustion dynamics, · Vol.2, No.1,* pp. 85–102, ISSN: 1756-8277

Kim, M. H. ; Lee, E. K. ; Jun, J. H. ; Kong, S. J. ; Han, G. Y. ; Lee, B. K. ; Lee, T. J. & Yoon, K. J. (2004). Hydrogen production by catalytic decomposition of methane over activated carbons: kinetic study. *International journal of hydrogen energy*, Vol. 29, No. 2, pp.187–93, ISSN: 0360-3199

Lambert, T. W.; Goodwin, V. M. ; Stefani, D. & Strosher, L.(2006). Hydrogen sulfide ($H_2S$) and sour gas effects on the eye. A historical perspective, *Journal of science of the total environment*, Vol. 367, pp.1–22, ISSN: 0048-9697

Lockwood, F. C. ; Niekerk, J. E. & Van J. E. (1995). Parametric study of a carbon black oil furnace, *Journal of combustion and flame*, Vol. 103, pp. 76-90, ISSN: 0010-2180

Moghiman, M. & Bashirnezhad, K. (2007). Experimental and numerical studies of carbon black natural gas furnace, *Kuwait journal of science and engineering*, Vol. 34; No. 1B, pp. 167-182, ISSN:1024-8684

Muradov, N. (2001). Catalysis of methane decomposition over elemental carbon. Journal of catalysis communications, Vol. 2, pp.89–94, ISSN: 1566-7367

Murthy, J. Y. & Mathur, S. R. (1998). Radiative heat Transfer in Axisymmetric Geometries using an Unstructured Finite-Volume Method, International journal of numerical heat transfer, Vol.33, No.4, pp.397-416, ISSN: 1040-7790

Petrasch, J. & Steinfeld, A. (2007). Dynamics of a solar thermochemical reactor for steam-reforming of methane, *Journal of chemical engineering science*, Vol. 62, pp. 4214-4228, ISSN: 1307- 6884

Ryu B. H., Lee S. Y., Lee D. H., Han Y., Lee J., Yoon J., Jang, J.S.; Kim, H.G.; Borse, P. H. & Lee, J. S. (2007). Simultaneous hydrogen production and decomposition of H2S dissolved in alkalinewater over CdS.TiO2 composite photocatalysts under visible light irradiation, *International journal of hydrogen energy*, Vol.32, pp. 4786-4791, ISSN: 0360-3199

Sakanishi, K. ; Wu, Z. ; Matsumura, A. & Saito, I.(2005). Simultaneous removal of $H_2S$ and COS using activated carbons and their supported catalysts, *Journal of catalysis today*, Vol.104, pp.94–100, ISSN: 0920-5861

Saario, A. & Rebola, A. (2005). Heavy fuel oil combustion in a cylindrical laboratory furnace: measurements and modeling, *Journal of fuel,* Vol.84, pp.359–369, ISSN: 0016-2361

Steinberg, M. (1998). Production of hydrogen and methanol from natural gas with reduced $CO_2$ emission. , *International journal of hydrogen energy*, Vol.23, No. 6, pp. 419-425, ISSN: 0360-3199

Towler, G. P. & Lynn, S. (1996). Sulfur recovery with reduced emissions, low capital investment and hydrogen co-production, *Journal of chemical engineering communications*, Vol. 155, 1996, pp. 113-143, ISSN: 0098-6445

T-Raissi, A. (2003). Analysis of Solar Thermochemical water-splitting cycles for hydrogen production, Hydrogen, Fuel Cells, and Infrastructure Technologies, FY 2003 Progress Report Available at : www.fsec.ucf.edu/en/research/hydrogen

Warnatz, J.; Maas, U. & Dibble, R.W., *Combustion*, Springer, ISBN: 3540259929 , Berlin (2006).

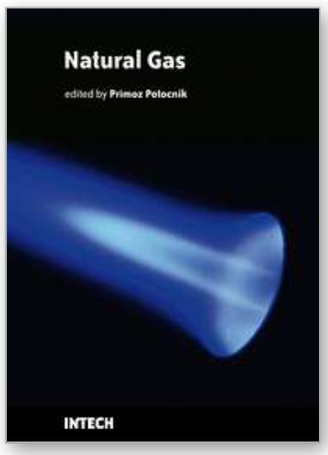


**Natural Gas**

Edited by Primoz Potocnik

ISBN 978-953-307-112-1

Hard cover, 606 pages

**Publisher** Sciyo

**Published online** 18, August, 2010

**Published in print edition** August, 2010

The contributions in this book present an overview of cutting edge research on natural gas which is a vital component of world's supply of energy. Natural gas is a combustible mixture of hydrocarbon gases, primarily methane but also heavier gaseous hydrocarbons such as ethane, propane and butane. Unlike other fossil fuels, natural gas is clean burning and emits lower levels of potentially harmful by-products into the air. Therefore, it is considered as one of the cleanest, safest, and most useful of all energy sources applied in variety of residential, commercial and industrial fields. The book is organized in 25 chapters that cover various aspects of natural gas research: technology, applications, forecasting, numerical simulations, transport and risk assessment.



**InTech Europe**

University Campus STeP Ri
Slavka Krautzeka 83/A
51000 Rijeka, Croatia
Phone: +385 (51) 770 447
Fax: +385 (51) 686 166
www.intechopen.com

**InTech China**

Unit 405, Office Block, Hotel Equatorial Shanghai
No.65, Yan An Road (West), Shanghai, 200040, China
中国上海市延安西路65号上海国际贵都大饭店办公楼405单元
Phone: +86-21-62489820
Fax: +86-21-62489821

IntechOpen